

# A study on the adequacy of common IQA measures for medical images

Anna Breger<sup>1,2\*</sup>, Clemens Karner<sup>2</sup>, Ian Selby<sup>3,4</sup>, Janek Gröhl<sup>5</sup>, Sören Dittmer<sup>1</sup>, Edward Lilley<sup>2</sup>, Judith Babar<sup>3,4</sup>, Jake Beckford<sup>4</sup>, Thomas R Else<sup>5</sup>, Timothy J Sadler<sup>4</sup>, Shahab Shahipasand<sup>4</sup>, Arthikkaa Thavakumar<sup>4</sup>, Michael Roberts<sup>1</sup>, and Carola-Bibiane Schönlieb<sup>1</sup>

<sup>1</sup> University of Cambridge, DAMTP, Cambridge, United Kingdom

<sup>2</sup> Medical University of Vienna, CMPBE, Vienna, Austria

<sup>3</sup> University of Cambridge, Department of Radiology, Cambridge, UK

<sup>4</sup> Cambridge University Hospitals, Department of Radiology, Cambridge, UK

<sup>5</sup> University of Cambridge, Department of Physics, Cambridge, UK

\*Corresponding author. E-mail: ab2864@cam.ac.uk

**Abstract.** Image quality assessment (IQA) is standard practice in the development stage of novel machine learning algorithms that operate on images. The most commonly used IQA measures have been developed and tested for natural images, but not in the medical setting. Reported inconsistencies arising in medical images are not surprising, as they have different properties than natural images. In this study, we test the applicability of common IQA measures for medical image data by comparing their assessment to manually rated chest X-ray (5 experts) and photoacoustic image data (2 experts). Moreover, we include supplementary studies on grayscale natural images and accelerated brain MRI data. The results of all experiments show a similar outcome in line with previous findings for medical imaging: PSNR and SSIM in the default setting are in the lower range of the result list and HaarPSI outperforms the other tested measures in the overall performance. Also among the top performers in our medical experiments are the full reference measures FSIM, GMSD, LPIPS and MS-SSIM. Generally, the results on natural images yield considerably higher correlations, suggesting that the additional employment of tailored IQA measures for medical imaging algorithms is needed.

**Keywords:** Image Quality · Medical Images · Quality Assessment.

## 1 Introduction

Advances in medical imaging technologies have been groundbreaking in the last decades, including the rapid development of deep learning techniques. To ensure the quality of novel image processing methodologies, quantitative image quality assessment (IQA) plays an important role in quality assurance in addition to visual inspection or even serves as the main assessment criterion when no expert opinion is available. Quantitative IQA can roughly be divided into three

categories based on their underlying assumptions and the information available for their evaluation [2, 28]. The first one is called full reference (FR) IQA, where a known full image is used as a reference and the quality of a given image is evaluated in a comparative way that relies on a meaningful notion of distance between the two images. No reference (NR) IQA aims to judge the quality without a reference based on pre-defined properties and reduced reference (RR) IQA uses derived image information of reference data.

Most common IQA measures have been developed for natural images and tested for specific tasks on a small amount of publicly available rated data sets. It is unknown how well these measures can be expanded to medical images since they have different properties including a different target space (color versus grayscale). Little research has been performed on the applicability of common IQA measures to medical imaging data, see e.g. [13] for a recent overview. Many prior applicability studies have limitations in the study design, including non-expert ratings (see e.g. [5]), non-realistic distortions (such as Gaussian additive noise, see e.g. [17]) and a very limited choice of IQA measures (see e.g. [21]). The research field is suffering from the lack of publicly available data sets with expert annotations for reproducible comparison studies, as well as code of introduced IQA measures.

Recently, in [13], the first extensive study on IQA measures comparing MRI outputs of image restoration models with expert ratings has been published. The results suggest that the most widely used measures PSNR [9] and SSIM [28] are not a good choice for the tested MRI tasks, which is in line with previous findings (see e.g. [4] for an overview of challenges when applying these measures to medical images). Here, we will build on that first study and assess the adequacy of common IQA measures for medical imaging in 4 different experimental setups and 5 data sets, including expert ratings for photoacoustic and chest X-ray data. For the comparisons we have included the following common IQA measures: peak signal-to-noise ratio (PSNR), structural similarity index measure (SSIM), multi-scale SSIM (MS-SSIM) [36], information content weighted SSIM (IW-SSIM) [29], deep image structure and texture similarity (DISTs) [8], DCT subband similarity (DSS) [3], feature similarity index (FSIM) [34], gradient magnitude similarity deviation (GMSD) [30], Haar wavelet-based perceptual similarity (HaarPSI) [20], learned perceptual image patch similarity (LPIPS) [35], mean deviation similarity (MDSI) [37], visual information fidelity (VIF) [24], and visual saliency-induced index (VSI) [33], in the FR setting; blind/referenceless image spatial quality evaluator BRISQUE [15], from patches to pictures (PaQ-2-PIQ) [31], and natural image quality evaluator (NIQE) [16] in the NR setting.

## 2 Methods

The IQA measures were computed with the implementations provided by their authors, either in MATLAB or Python, or both. An exception is the VIF measure for which we used the PyTorch Lightning implementation because the code by the authors is not publicly available. Reporting the implementation used is

of utmost importance because IQA results may differ substantially in regards to the implementation, see e.g. [27].

When novel manual image ratings were obtained (Experiment 1, 3, and 4), the novel publicly available speedyIQA annotation app [22] was used. The software asks the user to set a task and the rating categories, see Figure 1. Obtained ratings have been saved as a CSV file.

For the evaluation of the IQ measure performance we employed the Spearman Rank Correlation Coefficient (SRCC) and the Kendall Rank Correlation Coefficient (KRCC), which assess the ordinal association (rank) between the quality measures and the manual ratings. To account for the different scoring between multiple graders, we apply the z-score to the raw rating data of each grader and afterwards compute the mean, cf. [25]. For the evaluation, the absolute SRCC and KRCC between the z-score of the image ratings and the IQ values are stated.

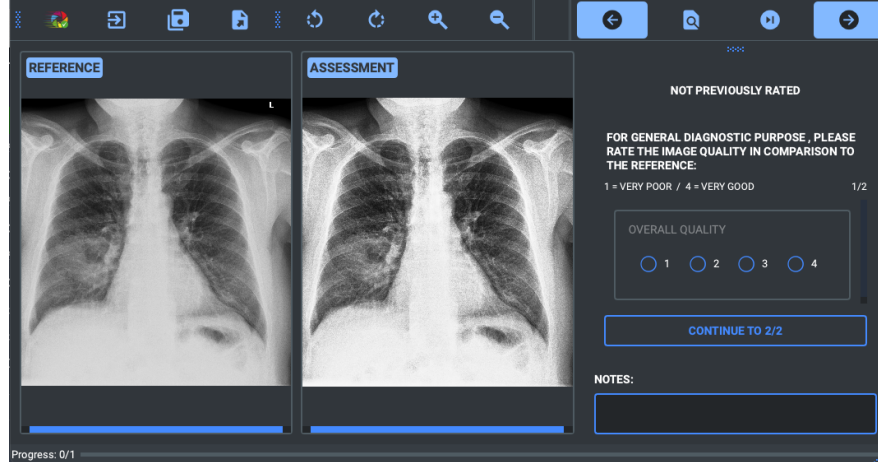


Fig. 1: The speedyIQA annotation app allows setting a task and rating categories for manual image ratings.

## 2.1 Experiment 1: Grayscale LIVE Data

The two data sets in the first experiment correspond to commonly used natural imaging quality assessment databases, namely the LIVE Image Quality Assessment Database Release 2 and the LIVE Multiply Distorted Image Quality Database [12, 23], which we transformed to grayscale images with the in-built MATLAB function *mat2gray*. The data sets contain respectively 982 and 405 images, including the degradations of Gaussian noise, jpeg compression, and blurring. Five volunteers were asked to rate all degraded images of both data sets from 1 (very poor), 2 (poor), 3 (good) to 4 (very good) regarding the ability to identify the detailed image content in comparison to the given reference image. Note that we did not use the original available color image ratings because

of the change in target space, see e.g. [20] for an example of inconsistencies related to grayscale versus color image ratings. Here, we asked the volunteers to rate the quality of the grayscale images regarding detailed image content. The annotations will be made available on github together with the implementation code of this evaluation study (<https://github.com/ideal-iqa/iqa-eval>).

## 2.2 Experiment 2: MRI Acceleration

The MRI data set was retrieved from the publicly available fastMRI brain dataset [32], which contains in total 6405 T1, T2, and FLAIR 3D k-space volumes. The fastMRI challenge series provided MRI datasets to foster the development of accelerated reconstruction algorithms. In [13] data from the fastMRI data set has been used for a comprehensive analysis of different degradations with expert annotations. Here, we use a subset of 4742 reference image slices (created by the root sum of squares, rSOS, of the fully sampled data) and around  $151k$  corresponding accelerated image reconstructions obtained from two machine learning algorithms that took part in the fastMRI multi-coil brain dataset challenge in 2020, namely the end-to-end variational network *E2E-VarNet* [26] and *XPDNet* [19]. *XPDNet* was among the top three submissions of the challenge and both algorithms perform very well on the corresponding public leaderboard. The reconstructions were obtained by the application of the machine learning models to the fully sampled and accelerated data, where we designed masks with acceleration factor 1 to 16 to yield decreasing visual image quality in the reconstructions, see Figure 2.

The created data set serves as a sanity check for the identification of decreasing image quality. We evaluate the performance of the IQA measures in two ways: First, the SRCC and KRCC are computed for each image and the corresponding quality decreases, where the acceleration factor serves as the image quality category, and secondly, we plot the mean IQA value for each acceleration class and measure. For this illustration, all measures are linearly scaled such that lower is always worse, starting with the IQA value of acceleration factor 1 as 100%. The purpose of this experiment is to test the IQA measure’s ability to flawlessly detect distinct quality decrease in medical images.

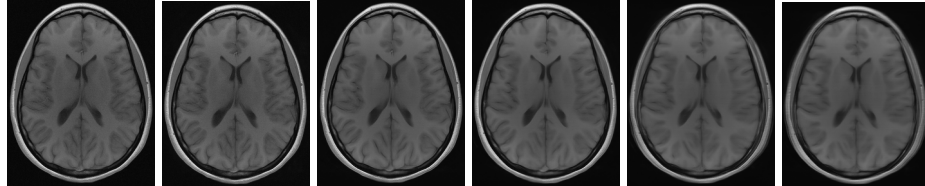


Fig. 2: Reconstructed MRI brain data from the fastMRI data set obtained with *E2E-VarNet* on the sub-sampled data with acceleration factors 1, 4, 8, 12 and 16. The left image corresponds to the reference image obtained via the rSOS of the fully sampled data. The visual quality decreases with the increased acceleration factor.

### 2.3 Experiment 3: Photoacoustic Reconstruction

Photoacoustic (PA) imaging is an emerging medical imaging modality with important clinical applications such as inflammatory bowel disease, cardiovascular diseases, and breast cancer [1]. The inverse problems of PAI pertain to accurately visualizing molecular distributions and determining functional tissue information from PA time series measurements [7]. We use a previously published open access data set, cf. [10], that consists of reconstructed images containing estimated distributions of the optical absorption coefficient from cross-sectional photoacoustic images of piecewise constant test objects (phantoms) [11]. The PA data were acquired with a commercial photoacoustic imaging system. The 378 reference images are obtained using a double-integrating sphere [18] setup as a complementary measurement system, which yields point estimates for homogeneous material samples. Because of the piecewise-constant nature of the used phantoms, one can fabricate an additional batch of the material used for the test object, measure it, and relate the calculated properties to the test object. This process is unfeasible for complicated objects or *in vivo* images, but can serve in this setting to obtain reference images.

Here, 1134 reconstructed images, corresponding to the outputs of 3 different reconstruction methods (see Figure 3), have been annotated by 2 experts. The experts were asked to rate the images from 1 (very poor), 2 (poor), 3 (good) to 4 (very good) regarding overall quality in comparison to the reference image without changing the contrast or luminance. For visualization and assessment, the outputs of the algorithms were clipped with the reference image's maximum. The annotations will be made available on Zenodo (<https://doi.org/10.5281/zenodo.13325197>).

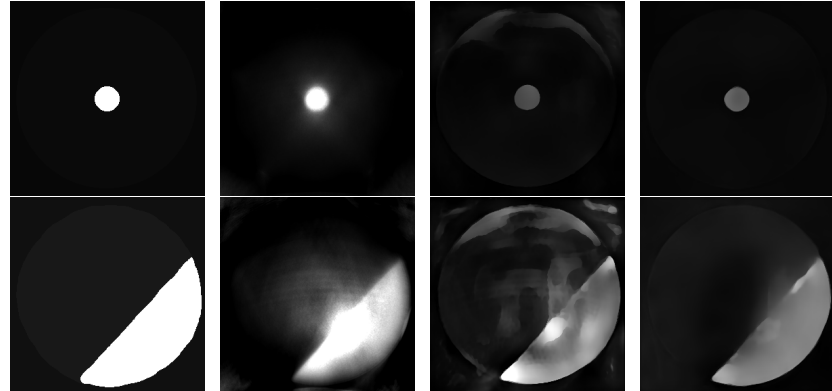


Fig. 3: Two examples of the photoacoustic images used, reference (left) and reconstructions from three algorithms. The first algorithm corrects a reconstructed PA image by using the light fluence obtained from simulations. The second and third algorithms are deep-learning models trained to estimate the absorption coefficient.

## 2.4 Experiment 4: Chest X-Ray Post-Processing

For the last experiment, we used posteroanterior chest radiographs that were acquired on two imaging systems (both Discovery XR656 HD models, GE Healthcare, USA) at Cambridge University Hospitals NHS Trust. Each scanner had previously been set up with different default post-processing parameters (chosen by local radiologists following a subjective assessment), yielding the reference images. Additional images, serving as real-life examples of lower quality, were produced for each radiographic exposure using multiple different post-processing settings, see examples in Figure 4. The post-processing was applied in the hospital directly on the scanner itself by adjusting parameters in the framework provided, including brightness, overall and tissue contrast, edge enhancement, noise reduction, and local contrast enhancement. In total, the data set contains 444 reference images and 2018 post-processed images that were rated by 3 consultant radiologists, 1 trainee radiologist, and 1 senior reporting radiographer. Each expert was asked to rate all post-processed images from 1 (very poor), 2 (poor), 3 (good) to 4 (very good) for general diagnostic purposes in comparison to the reference without changing the contrast or luminance of the displayed image. The image data and annotations are in progress to be made available in a managed way in accordance with the ethical agreements of the acquired clinical data.



Fig. 4: Chest X-ray scans with different kinds of post-processing, the image on the left serves as the reference, the other images show lower visual quality.

## 3 Results and Discussion

An important problem regarding fairness in machine learning is the adequacy of employed assessment methods. In the context of IQA measures, this relates to the question of generalizability across different datasets and image target spaces. To tackle this question, we conducted 4 independent experiments, where on the one hand 4 novel data sets were obtained with manual expert ratings and on the other hand 1 data set was designed to test the ability to identify obvious quality decrease in medical images. For the comparison we chose IQA measures that are commonly used across image modalities and tasks. The results of Experiment 2 (see Figure 5) show that all tested FR measures were able to pass the sanity check, i.e. they were able to identify the distinct decrease in quality of the MRI

Full-Reference	Grayscale Natural Images		Medical Images	
	LIVE	LIVE <sub>Multi</sub>	Photoacoustic	Chest X-ray
PSNR	0.87 / 0.71	0.74 / 0.56	0.65 / 0.47	0.66 / 0.48
SSIM	0.88 / 0.72	0.67 / 0.49	0.69 / 0.54	0.70 / 0.50
SSIM*	0.88 / 0.71	0.67 / 0.49	0.70 / 0.54	0.70 / 0.50
MS-SSIM	0.91 / 0.77	0.88 / 0.70	<b>0.83/0.67</b>	0.80 / 0.58
MS-SSIM*	0.91 / 0.76	0.88 / 0.71	0.82 / 0.66	0.79 / 0.57
IW-SSIM	0.92 / 0.79	<b>0.93/0.77</b>	0.76 / 0.59	0.72 / 0.52
DISTS	0.91 / 0.76	0.75 / 0.56	0.78 / 0.61	0.77 / 0.54
DISTS*	0.91 / 0.76	0.74 / 0.56	0.77 / 0.60	0.77 / 0.55
DSS	0.92 / 0.78	0.91 / 0.74	0.77 / 0.60	0.68 / 0.50
FSIM	<b>0.93/0.80</b>	0.92 / 0.75	<b>0.80/0.64</b>	0.79 / 0.56
GMSD	<b>0.92/0.79</b>	0.91 / 0.74	0.78 / 0.61	0.82 / 0.61
HaarPSI	<b>0.93/0.79</b>	<b>0.92/0.76</b>	<b>0.81/0.65</b>	<b>0.83/0.61</b>
LPIPS* <sub>Alex</sub>	0.90 / 0.75	0.77 / 0.59	0.78 / 0.62	<b>0.82/0.62</b>
MDSI	0.92 / 0.78	<b>0.92/0.76</b>	0.67 / 0.50	0.76 / 0.53
VIF*	0.85 / 0.68	0.90 / 0.72	0.19 / 0.14	0.63 / 0.43
VSI	0.91 / 0.77	0.89 / 0.71	0.04 / 0.02	<b>0.83/0.62</b>
<i>No-Reference</i>				
BRISQUE	0.92 / 0.78	0.46 / 0.33	0.70 / 0.53	0.05 / 0.03
NIQE	0.88 / 0.71	0.75 / 0.57	0.58 / 0.42	0.44 / 0.30
PAQ-2-PIQ*	0.76 / 0.57	0.86 / 0.68	0.20 / 0.14	0.59 / 0.41

Table 1: SRCC/KRCC of all tested IQA measures and the mean of the rated images' z-scores, described in Section 2 in Experiment 1, 3, 4. The top 3 performers have been printed in bold for each data set. Measures marked with \* have been computed with implementations provided by the authors in Python, for all other measures the provided MATLAB implementations were used. PSNR and HaarPSI provided in both implementations identical results.

images, confirmed through the descending mean quality value as well as the high SRCC/KRCC values related to the acceleration categories. Two of the tested NR measures, NIQE and PAQ-2-PIQ, struggled to correctly identify the decreasing image quality.

In Table 1 we show the SRCC and KRCC values for the tested IQA measures and the 4 manually rated data sets of Experiments 1, 3 and 4. The commonly used measures PSNR and SSIM yield relatively low correlation values in all tasks, especially regarding the medical imaging data sets. Outstanding behavior is shown by HaarPSI which is among the top 3 performers for all tested data sets. Generally, the correlation values for the natural images are higher than for the medical images, indicating that improvement is still needed in the medical domain and tailored available measures should be employed for specified tasks. The reasons for that are manifold. On the one hand, most of the tested measures have been developed and calibrated for natural images, and on the other hand, medical imaging tasks are often very complex or ask for specific quality information. Strongly dependent on the task, different image features might be more or less important.

The tested FR measures yield higher correlation coefficients than the NR mea-

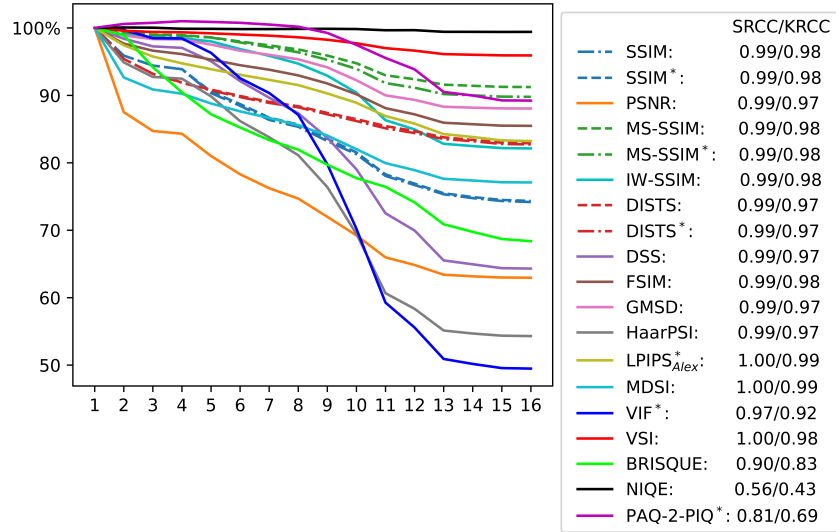


Fig. 5: IQA comparison of decreasing MRI reconstruction quality through an increase in acceleration factor (1 to 16). All tested FR measures correctly identify a decrease in quality, two of the tested NR measures (NIQE and PAQ-2-PIQ) struggle to identify the quality loss accurately. The SRCC/KRCC values between the measures and the acceleration categories show corresponding behavior.

sures, which is not surprising as FR assessment is using more information. In the NR setting, recently, measures tailored towards assessment of specific medical images have been introduced, see e.g. [6, 14], and it is advisable to employ such measures in medical imaging tasks, in addition to more generalizable measures. Using unsuitable IQA measures might give incorrect conclusions about novel introduced algorithms, not necessarily favoring the most adequate methods.

## 4 Conclusion

We systematically test the ability of common FR and NR IQA measures to assess the quality of medical images and find that all measures correlate less with expert assessment of medical images compared to grayscale natural images. Even though PSNR and SSIM are commonly used across fields, they yield relatively low results, confirming previous studies that these two measures are not beneficial to assess medical imaging tasks and emphasizing the need to employ specifically task-targeted IQ measures. On the other hand, HaarPSI showed exceptional behavior regarding generalizability, suggesting it acts as a robust measure of quality in addition to such specifically tailored measures. FSIM, GMSD and MS-SSIM also showed relatively robust successful behavior across the data sets; LPIPS and DIST succeeded in most tasks.

In summary, we present a comprehensive study to assess the adequacy of com-

mon IQA measures in medical imaging tasks including rated chest X-ray scans and photoacoustic images. We show the dire need for better suited IQA measures and hope to provoke more research in this direction, including more extensive suitability studies as well as further implementations of task-tailored measures.

## References

1. Assi, H., Cao, R., et al: A review of a strategic roadmapping exercise to advance clinical translation of photoacoustic imaging: From current barriers to future adoption. *Photoacoustics* **32**, 100539 (2023). <https://doi.org/https://doi.org/10.1016/j.pacs.2023.100539>
2. Athar, S., Wang, Z.: A comprehensive performance evaluation of image quality assessment algorithms. *IEEE Access* **7**, 140030–140070 (09 2019). <https://doi.org/10.1109/ACCESS.2019.2943319>
3. Balanov, A., Schwartz, A., Moshe, Y., Peleg, N.: Image quality assessment based on dct subband similarity. In: 2015 IEEE International Conference on Image Processing (ICIP). pp. 2105–2109 (2015). <https://doi.org/10.1109/ICIP.2015.7351172>
4. Breger, A., Biguri, A., Landman, M.S., Selby, I., Amberg, N., Brunner, E., Gröhl, J., Hatamikia, S., Karner, C., Ning, L., Dittmer, S., Roberts, M., Collaboration, A.C., Schönlieb, C.B.: A study of why we need to reassess full reference image quality assessment with medical images. *ArXiv preprint arXiv:2405.19097* (May 2024)
5. Chow, L.S., Rajagopal, H., Paramesran, R.: Correlation between subjective and objective assessment of magnetic resonance (mr) images. *Magn Reson Imaging* **34**(6), 820–831 (Jul 2016). <https://doi.org/10.1016/j.mri.2016.03.006>
6. Chun, M., Choi, J.H., Kim, S., Ahn, C., Kim, J.H.: Fully automated image quality evaluation on patient ct: Multi-vendor and multi-reconstruction study. *PLoS One* **17**(7), e0271724 (2022). <https://doi.org/10.1371/journal.pone.0271724>
7. Cox, B., Laufer, J.G., Arridge, S.R., Beard, P.C.: Quantitative spectroscopic photoacoustic imaging: a review. *J Biomed Opt* **17**(6), 061202 (Jun 2012). <https://doi.org/10.1117/1.JBO.17.6.061202>
8. Ding, K., Ma, K., Wang, S., Simoncelli, E.P.: Image quality assessment: Unifying structure and texture similarity. *IEEE Transactions on Pattern Analysis and Machine Intelligence* **44**(5), 2567–2581 (2022). <https://doi.org/10.1109/TPAMI.2020.3045810>
9. Girod, B.: Psychovisual aspects of image processing: What's wrong with mean squared error? In: Proceedings of the Seventh Workshop on Multidimensional Signal Processing. pp. P.2–P.2 (1991). <https://doi.org/10.1109/MDSP.1991.639240>
10. Gröhl, J., Else, T., Hacker, L., Bunce, E., Sweeney, P., Bohndiek, S.: Dataset for: Moving beyond simulation: data-driven quantitative photoacoustic imaging using tissue-mimicking phantoms (2023), <https://doi.org/10.17863/CAM.96644>
11. Grohl, J., Else, T.R., Hacker, L., Bunce, E.V., Sweeney, P.W., Bohndiek, S.E.: Moving beyond simulation: data-driven quantitative photoacoustic imaging using tissue-mimicking phantoms. *IEEE Trans Med Imaging* **PP** (Nov 2023). <https://doi.org/10.1109/TMI.2023.3331198>
12. Jayaraman, D., Mittal, A., Moorthy, A.K., Bovik, A.C.: Objective quality assessment of multiply distorted images. In: 2012 Conference Record of the Forty Sixth Asilomar Conference on Signals, Systems and Computers (ASILOMAR). pp. 1693–1697 (2012). <https://doi.org/10.1109/ACSSC.2012.6489321>

13. Kastrulyina, S., Zakirov, J., Pezzotti, N., Dylov, D.V.: Image quality assessment for magnetic resonance imaging. Elsevier Medical Image Analysis (2022). <https://doi.org/10.1109/ACCESS.2023.3243466>
14. Lei, K., Syed, A.B., Zhu, X., Pauly, J.M., Vasanawala, S.S.: Artifact- and content-specific quality assessment for mri with image rulers. Medical Image Analysis **77**, 102344 (2022). <https://doi.org/https://doi.org/10.1016/j.media.2021.102344>
15. Mittal, A., Moorthy, A.K., Bovik, A.C.: No-reference image quality assessment in the spatial domain. IEEE Transactions on Image Processing **21**(12), 4695–4708 (2012). <https://doi.org/10.1109/TIP.2012.2214050>
16. Mittal, A., Soundararajan, R., Bovik, A.C.: Making a “completely blind” image quality analyzer. IEEE Signal Processing Letters **20**(3), 209–212 (2013). <https://doi.org/10.1109/LSP.2012.2227726>
17. Ohashi, K., Nagatani, Y., Yoshigoe, M., Iwai, K., Tsuchiya, K., Hino, A., Kida, Y., Yamazaki, A., Ishida, T.: Applicability evaluation of full-reference image quality assessment methods for computed tomography images. Journal of Digital Imaging **36**(6), 2623–2634 (2023). <https://doi.org/10.1007/s10278-023-00875-0>
18. Pickering, J.W., Prahl, S.A., van Wieringen, N., Beek, J.F., Sterenborg, H.J.C.M., van Gemert, M.J.C.: Double-integrating-sphere system for measuring the optical properties of tissue. Appl. Opt. **32**(4), 399–410 (Feb 1993). <https://doi.org/10.1364/AO.32.000399>
19. Ramzi, Z., Ciuciu, P., Starck, J.L.: XPDNet for MRI Reconstruction: an application to the 2020 fastMRI challenge. In: ISMRM. pp. 1–4 (2021)
20. Reisenhofer, R., Bosse, S., Kutyniok, G., Wiegand, T.: A haar wavelet-based perceptual similarity index for image quality assessment. Signal Process. Image Commun. **61**, 33–43 (2018). <https://doi.org/10.1016/j.image.2017.11.001>
21. Renieblas, G.P., Nogués, A.T., González, A.M., Gómez-Leon, N., Del Castillo, E.G.: Structural similarity index family for image quality assessment in radiological images. J Med Imaging (Bellingham) **4**(3), 035501 (Jul 2017). <https://doi.org/10.1117/1.JMI.4.3.035501>
22. Selby, I.: Github repository speedyiq (March 2024), [https://github.com/selbs/speedy\\_iqa](https://github.com/selbs/speedy_iqa)
23. Sheikh, H.R., Wang, Z., Cormack, L., Bovik, A.C.: Live image quality assessment database release 2 (<http://liveeceutexasedu/research/quality>), <http://live.ece.utexas.edu/research/quality>
24. Sheikh, H., Bovik, A.: A visual information fidelity approach to video quality assessment. The First International Workshop on Video Processing and Quality Metrics for Consumer Electronics (2005)
25. Sheikh, H., Sabir, M., Bovik, A.: A statistical evaluation of recent full reference image quality assessment algorithms. IEEE Transactions on Image Processing **15**(11), 3440–3451 (2006). <https://doi.org/10.1109/TIP.2006.881959>
26. Sriram, A., Zbontar, J., Murrell, T., Defazio, A., Zitnick, C.L., Yakubova, N., Knoll, F., Johnson, P.: End-to-end variational networks for accelerated mri reconstruction. In: Medical Image Computing and Computer Assisted Intervention–MICCAI 2020: 23rd International Conference, Lima, Peru, October 4–8, 2020, Proceedings, Part II 23. pp. 64–73. Springer (2020)
27. Venkataramanan, A.K., Wu, C., Bovik, A.C., Katsavounidis, I., Shahid, Z.: A hitchhiker’s guide to structural similarity. IEEE Access **9**, 28872–28896 (2021). <https://doi.org/10.1109/ACCESS.2021.3056504>
28. Wang, Z., Bovik, A., Sheikh, H., Simoncelli, E.: Image quality assessment: from error visibility to structural similarity. IEEE Transactions on Image Processing **13**(4), 600–612 (2004). <https://doi.org/10.1109/TIP.2003.819861>

29. Wang, Z., Li, Q.: Information content weighting for perceptual image quality assessment. *IEEE Transactions on Image Processing* **20**(5), 1185–1198 (2011). <https://doi.org/10.1109/TIP.2010.2092435>
30. Xue, W., Zhang, L., Mou, X., Bovik, A.C.: Gradient magnitude similarity deviation: A highly efficient perceptual image quality index. *IEEE Transactions on Image Processing* **23**(2), 684–695 (2014). <https://doi.org/10.1109/TIP.2013.2293423>
31. Ying, Z., Niu, H., Gupta, P., Mahajan, D., Ghadiyaram, D., Bovik, A.: From patches to pictures (paq-2-piq): Mapping the perceptual space of picture quality. pp. 3572–3582 (06 2020). <https://doi.org/10.1109/CVPR42600.2020.00363>
32. Zbontar, J., Knoll, F., Sriram, A., Murrell, T., Huang, Z., Muckley, M.J., Defazio, A., Stern, R., Johnson, P., Bruno, M., Parente, M., Geras, K.J., Katsnelson, J., Chandarana, H., Zhang, Z., Drozdza, M., Romero, A., Rabbat, M., Vincent, P., Yakubova, N., Pinkerton, J., Wang, D., Owens, E., Zitnick, C.L., Recht, M.P., Sodickson, D.K., Lui, Y.W.: fastmri: An open dataset and benchmarks for accelerated mri (2019)
33. Zhang, L., Shen, Y., Li, H.: Vsi: A visual saliency-induced index for perceptual image quality assessment. *IEEE Transactions on Image Processing* **23**(10), 4270–4281 (2014). <https://doi.org/10.1109/TIP.2014.2346028>
34. Zhang, L., Zhang, L., Mou, X., Zhang, D.: Fsim: A feature similarity index for image quality assessment. *IEEE Transactions on Image Processing* **20**(8), 2378–2386 (2011). <https://doi.org/10.1109/TIP.2011.2109730>
35. Zhang, R., Isola, P., Efros, A.A., Shechtman, E., Wang, O.: The unreasonable effectiveness of deep features as a perceptual metric. In: 2018 IEEE/CVF Conference on Computer Vision and Pattern Recognition. pp. 586–595 (2018). <https://doi.org/10.1109/CVPR.2018.00068>
36. Zhou Wang, E.P.S., Bovik, A.C.: Multi-scale structural similarity for image quality assessment. In: Proceedings of the 37th IEEE Asilomar Conference on Signals, Systems and Computers, Pacific Grove, CA (2003)
37. Ziae Nafchi, H., Shahkolaei, A., Hedjam, R., Cheriet, M.: Mean deviation similarity index: Efficient and reliable full-reference image quality evaluator. *IEEE Access* **4**, 5579–5590 (2016). <https://doi.org/10.1109/ACCESS.2016.2604042>